BNL-26989

CONF-791102--86

MASTER

AN ANALYSIS OF CRITICAL CURRENT-BEND STRAIN RELATIONSHIPS IN COMPOSITE Nb_3Sn SUPERCONDUCTING WIRES

Thomas Luhman and D. O. Welch
Brookhaven National Laboratory
Upton, New York 11973

BNL-26989

AN ANALYSIS OF CRITICAL CURRENT-BEND STRAIN RELATIONSHIPS IN COMPOSITE Nb_3Sn SUPERCONDUCTING WIRES*

Thomas Luhman and D. O. Welch†

ABSTRACT

In order to be used successfully in fusion magnets, Nb_3Sn conductors must meet several mechanical strain criteria, including tolerance to bending strains encountered during magnet construction. Since Nb_3Sn is extremely brittle much information has been generated regarding the sensitivity of these conductors to tensile strain. A recent comparison of critical current-bend and tensile test data indicates that the strain required to initiate compound cracking during bending is significantly less than the strain required to do so by tensile straining [1]. In the present paper, the dependence of critical current on bending strains in monofilamentary Nb_3Sn wires is calculated and compared with experimental data. The calculation takes into account a shift in the composite's neutral axis which occurs during bending. The analysis correctly predicts the observed dependence of the critical current on bending strains.

I. INTRODUCTION

The limited strain tolerances of Nb_3Sn conductors generally restricts their use to strain margins of less than 0.6-0.8% [2]. Within this range the critical superconducting properties (J_c, T_c, and H_{c2}) depend on strain [2]. Therefore, in order to consider a conductor for a particular magnet design it is necessary to know how its superconducting properties vary with applied strain. In this regard both tensile and bending strains are important. Owing to the difficulty of making bend tests (small strains require very large bore magnets) it is of interest to be able to forecast bend strain behavior from tensile strain data. Recent work on a series of monofilamentary conductors revealed that their tolerance to bending strains was significantly less than their tensile strain tolerances [1]. A qualitative explanation based on a shift occurring in the conductor's neutral axis during bending satisfactorily described the observations. The shift occurs as a result of plastic yielding in the bronze matrix induced by the combination of applied bending strains and residual internal strains present in as-heat treated conductors. The residual internal strains take the form of tension in the bronze matrix and compression in the core. The total strain resulting from the sum of the applied tensile and residual tensile strains in the outer dimensions of the matrix (tensile zone in bending) is sufficient to produce plastic flow in this region prior to plastic flow in the compression zone. The plastic flow unbalances the forces in the conductor's cross section and results in a shift of the conductor's neutral axis toward the center of bend curvature.

In the present paper we show that the bend strain-critical current relationship for these monofilamentary conductors can be calculated from tensile test data when the neutral axis shift is taken into account. Using experimentally determined tensile cracking strains for the Nb_3Sn compound layer, good agreement is obtained between calculated current densities and experimental bend test data.

Calculation of J_c as a Function of Bending Strains

In a monofilamentary conductor the Nb_3Sn compound may be represented as a cylinder of radius R and thickness t. If the composite behaves elastically, the applied bending strain, ε_b, in a particular element of the conductor at a height Z above the center of the cylinder is given by Z/ρ where ρ is the bend radius; the maximum bending strain in the Nb_3Sn is $R/\rho \equiv \varepsilon_s$. This representation of bending strain does not include a shift in the neutral axis, assuming rather that the neutral axis and geometric center of the conductor coincide. When a shift in the neutral axis Δr occurs because of plasticity in the bronze, the true bending strain in the conductor, ε_t, can be written as $\varepsilon_b+(\Delta r/\rho)$ or $\varepsilon_b+\varepsilon_o$, letting $\Delta r/\rho$ equal ε_o (a strain representation of the neutral axis shift). In the discussion to follow, we will characterize the severity of bending by the apparent maximum bending strain $\varepsilon_s \equiv R/\rho$, recognizing that this must be corrected for the neutral axis shift to obtain the true maximum bending strain. The total strain in the conductor, ε, is a sum of the true applied bending strain, ε_t, and the internal strain, $-\varepsilon_i$, built in during the fabrication of the composite. The critical current depends upon the total strain.

The approach taken is to consider a conductor subjected to bending deformation, to calculate the strain distribution due to the applied bending strain (including the neutral axis shift) and the internal strain, and to average the strain dependent critical current density over the cross sectional area of the compound layer. The following assumptions are made. It is assumed that once ε reaches the tensile cracking strain of the compound, ε_f^T, that particular portion of the superconductor no longer carries superconducting current. The value of ε_f^T is obtained from tensile test data where $\varepsilon_f^T = \varepsilon_a^T - \varepsilon_i$. Here ε_a^T is the applied tensile strain and ε_i the internal residual compressive strain on the Nb_3Sn compound; $\varepsilon_a^T = \varepsilon_i$ at the peak in a tensile strain - J_c plot. A second assumption is that the critical current in the region where the compound hasn't cracked is an average value given by:

$$I_c = t \int_{\substack{\text{uncracked} \\ \text{region}}} J_c[\varepsilon(\ell)]\,d\ell \qquad (1)$$

where $d\ell$ is taken along the circumference of the cylindrical layer. The critical current density is explicitly a function of the total elastic strain and thus is implicitly a function of the location on the layer.

The dependence of J_c on strain is known from tensile test data. Figure 1 presents this data for the series of monofilamentary conductors used in these experiments. The experimental procedures employed to collect this data are detailed in Ref. 3. The critical current is normalized to its maximum value and strain is plotted as intrinsic strain where the assumption is made that the net strain on the conductor is zero at the maximum in J_c. For the purpose of the present calculation the J_c-ε data of Fig. 1 is represented by two linear functions; for the compressive and tensile strain domains

$$J_c(\varepsilon) = -a\varepsilon + J_{max} \qquad \varepsilon>0$$

$$J_c(\varepsilon) = +a\varepsilon + J_{max} \qquad \varepsilon<0$$

The neutral axis shift is taken to be a linear function of the maximum applied bending strain, i.e., $\varepsilon_o = \phi\varepsilon_s$ where

---

*Work supported by DOE.

†Brookhaven National Lab., Upton, New York 11973.

ϕ is assumed to be a constant. A determination of the applied bending strain at fracture, ε_s^f, yields the neutral axis shift at fracture, $\varepsilon_o^f = \varepsilon_f^T + \varepsilon_i - \varepsilon_s^f$, and thus $\phi = \varepsilon_o^f/\varepsilon_s^f$.

Substituting the linear J_c–ε relationships and the calculated strain distribution including the neutral axis shift into Eq (1) and integrating yields several stages of behavior with increasing ε_s:

Stage 1: $\varepsilon_s \leq \frac{\varepsilon_i}{(1+\phi)}$

$$I_c/I_1 = 1 + \frac{a\phi}{J_1}\varepsilon_s \tag{3}$$

Stage 2: $\frac{\varepsilon_i}{(1+\phi)} < \varepsilon_s \leq \frac{\varepsilon_f+\varepsilon_i}{(1+\phi)}$

$$\frac{I_c}{I_1} = \left(1+\frac{a\varepsilon_i}{J_1}\right) - \frac{2}{\pi}\frac{a}{J_1}(\varepsilon_i - \phi\varepsilon_s)\sin^{-1}\left(\frac{\varepsilon_i}{\varepsilon_s} - \phi\right)$$
$$- \frac{2a\varepsilon_s}{\pi J_1}\left[1 - \left(\frac{\varepsilon_i}{\varepsilon_s} - \phi\right)^2\right]^{1/2} \tag{4}$$

Stage 3: $\frac{\varepsilon_f+\varepsilon_i}{(1+\phi)} < \varepsilon_s$

$$\frac{I_c}{I_1} = \frac{1}{\pi}\left\{1 + \frac{a}{J_1}(2\varepsilon_i - \phi\varepsilon_s)\right\}\sin^{-1}\left(\frac{\varepsilon_i+\varepsilon_f}{\varepsilon_s} - \phi\right)$$
$$- \frac{2}{\pi}\frac{a}{J_1}(\varepsilon_i - \phi\varepsilon_s)\sin^{-1}\left(\frac{\varepsilon_i}{\varepsilon_s} - \phi\right)$$
$$+ \frac{a\varepsilon_s}{\pi J_1}\left[1 - \left(\frac{\varepsilon_i+\varepsilon_f}{\varepsilon_s} - \phi\right)^2\right]^{1/2}$$
$$- \frac{2a\varepsilon_s}{\pi J_1}\left[1 - \left(\frac{\varepsilon_i}{\varepsilon_s} - \phi\right)^2\right]^{1/2}$$
$$+ \frac{1}{2}\left(1 + \frac{a\phi}{J_1}\varepsilon_s\right) \tag{5}$$

where I_1 is the initial as-heat treated value of the critical current, and J_1 the critical current density.

Stage 1 represents the variation of I_c when the "true" applied strain, $\varepsilon_t = \varepsilon_s + \varepsilon_o$, is less than the internal residual compressive strain ε_i. Due to the assumption in Eq (2), the critical current in Stage 1 has a linear dependence on the applied strain ε_s. As ε_t exceeds ε_i the conductor enters Stage 2 where the critical current density associated with the maximum tensile strain in the compound begins to decrease. The peak in I_c occurs during stage 2. When ε_t reaches $(\varepsilon_i + \varepsilon_f^T)$ the conductor enters Stage 3, characterized by cracking of the compound layer wherever the maximum tensile strain equals ε_f^T. Stage 3 contains contributions to I_c determined by a wide range of strain values from the maximum compression value to ε_f^T.

Comparison with Experimental Data

A compilation of the experimental data is presented in Table I for the series of monofilamentary conductors. The bronze-to-niobium ratios, R_v, vary from 1.95 to 58. The values of a/J_1 were determined from Fig. 1 where the applied magnetic field was 4T. Figures 2-6 compare the experimental bend test data at 4T with the critical current-bend strain relationships calculated from Eqs. (3), (4), and (5). (In these figures the dashed portion of the curves represent calculated I_c-applied bending strain behavior assuming compound cracking does not occur, i.e., an extension of Stage 2 to higher applied strains.) At each value of R_v the calculated curves closely approximate the experimental bend test data, with ϕ being the only fitted parameter. For example, the applied bending strain for which compound cracking will occur, and the associated precipitous drop in I_c, is seen in the calculated curve and the experimental data at nearly the same applied strain. Other features of the experimental data are also exhibited in the calculated curves. The values of strain associated with the peak in I_c/I_1 increase with increasing R_v. The magnitude of the peak in I_c/I_1 shows a maximum value at $R_v = 7.6$ and then decreases continuously to minimum values at the extreme ranges of R_v, 1.95 and 58. These features of the I_c-bend strain behavior have been fully described in previous work [1]. Briefly, the increase in strain associated with the peak in I_c/I_1 reflects an increasing amount of residual compressive strain, ε_i, with increasing R_v. Thus a larger applied strain is required to counterbalance ε_i. A maximum in I_c/I_1 occurs when a shift in the neutral axis places more than 50% of the conductor's cross sectional area in tension. The maximum in the magnitude of I_c/I_1 at $R_v = 7.6$ is associated with the largest neutral axis shift (note Table I) and hence at this value of R_v, a maximum percentage of the conductor's cross section is placed in tension.

In general the predicted values of I_c/I_1 are 5-10% higher than the experimental data. This is probably related to the assumption of linearity between I_c and strain, Eq (2). Such an assumption implies I_c values, near an intrinsic strain of zero, that are ~5-10% high. Use of a quadratic function should therefore improve this aspect of the correlation with experimental data.

The present calculations were done for bend tests at 4T. It is possible to extend the predicted bend test behavior of I_c to other magnetic fields. The magnetic field dependence enters the calculation through the parameter a/J_1, where the symbol a represents the slope of an I_c-tensile strain plot like that in Fig. 1. The magnitude of this slope increases as the magnetic field increased [4]. Figure 7 presents the parameter a/J_1 as a function of magnetic field. The data in this figure include those for the monofilamentary conductors of the present work as well as for a 1615 filament conductor [4]. The curve is representative of stoichiometric Nb_3Sn, the multifilament conductor having been heat treated for 16 h at 700°C, [4] the monofilament material 15 h at 725°C. Using this approach the I_c-bend strain behavior can be predicted as a function of applied magnetic field. The major effect would be an increase in the magnitude of I_c/I_1 at its peak value in the strain curve. Parameters such as the cracking strain and residual prestrain would not be affected.

CONCLUSIONS

The I_c-bend strain behavior for a series of monofilamentary conductors has been predicted from I_c-tensile strain measurements. Inclusion of the neutral axis shift which occurs as a consequence of plastic flow in the bronze matrix during bending is essential to account for the observed differences between compound cracking strains in tension and bend tests. In general the major features of the bend test data are revealed in the calculated curves. One source of error in the calculation is the assumption of a linear, rather than quadratic, relationship between I_c and tensile strain. Work is currently underway to include a quadratic relationship in the calculation, as well as to extend the calculation to multifilamentary geometries. Predicting I_c-bend strain relationships at magnetic fields other than those for which I_c-tensile strain data is available should be possible providing a measure of the parameter a/J_1 is available.

ACKNOWLEDGMENTS

The authors are grateful to their colleages M. Suenaga and K. Aihara for stimulating discussions on

this topic. We wish to fully acknowledge the illuminating assistance from K. Kaiho, both experimental and theoretical, on all aspects of this work. The technical aid of F. Perez is also very much appreciated.

REFERENCES

[1] K. Kaiho, T. S. Luhman, M. Suenaga, and W. B. Sampson, accepted for publication in Appl. Phys. Letts., 1979.

[2] For general references see; IEEE Trans. on Magnetics, Vol. MAG-15, 1979, 13-1977, and 11-1975; Advances in Cryogenic Eng., Vol. 24, 1977 and Vol. 22, 1975.

[3] Thomas Luhman, M. Suenaga, D. O. Welch, and K. Kaito, IEEE Trans. on Magnetics, Vol. MAG-15, No. 1, p. 697.

[4] G. Rupp, IEEE Trans. on Magnetics, Vol. MAG-15, No. 1, p. 189, 1979.

Table 1

SUMMARY OF TENSILE AND BEND TEST DATA FOR A SERIES OF MONOFILAMENTARY CONDUCTORS
(Also Included are Pertinent Parameters Associated with the Calculation of I_c-Bending Strain Behavior)

							Calculated		
R_v	ε_i	$\frac{a}{J_I}$	$\varepsilon_o^f = \varepsilon_f^T + \varepsilon_i - \varepsilon_s^f$	$\phi = \frac{\varepsilon_o^f}{\varepsilon_s^T}$	$\mu = \frac{a\varepsilon_i}{J_I}$	$e_f = \frac{\varepsilon_f^T}{\varepsilon_i}$	$\frac{I_c}{I_1}(\max) = 1 + \frac{\mu\phi}{1+\phi}$	Stage II Onset	Stage III Onset
1.95	0.4	0.29	0.45	0.75	0.116	$\frac{0.6}{0.4}=1.5$	1.05	0.23	0.58
2.76	0.6	0.31	0.5	1.0	0.186	$\frac{0.5}{0.6}=0.83$	1.09	0.3	0.55
7.6	0.9	0.36	0.55	1.22	0.324	$\frac{0.45}{0.9}=0.5$	1.18	0.41	0.60
13.5	1.0	0.38	0.25	0.71	0.38	$\frac{0.35}{1.0}=0.35$	1.16	0.59	0.80
58	1.0	0.38	0.1	0.33	0.42	$\frac{0.3}{1}=0.3$	1.1	0.75	1.2

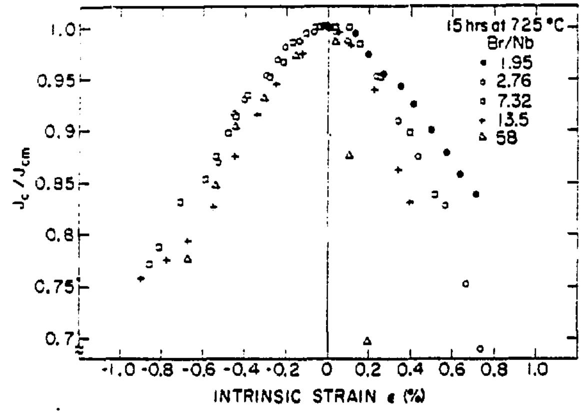

Figure 1. Tensile Strain-I_c data for a series of monofilamentary conductors, 4T, 4.2K.

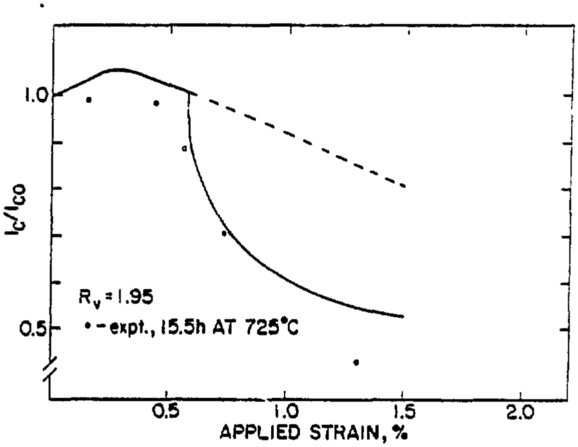

Figure 2. Calculated and observed critical current as a function of applied bending strain. Samples were bend at room temperature and tested for their current carrying capacities at 4.2K and 4T.

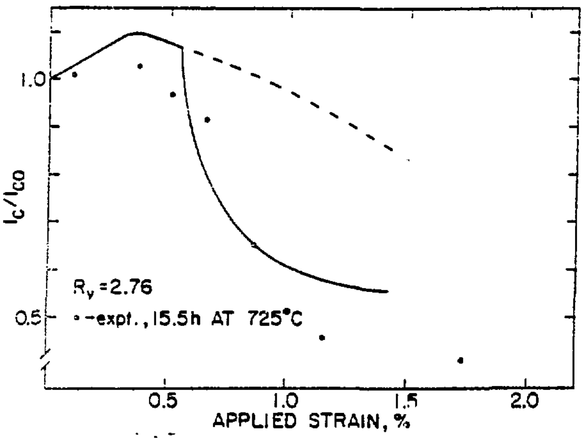

Figure 3. Calculated and observed critical current as a function of applied bending strain. Samples were bent at room temperature and tested for their current carrying capacities at 4.2K and 4T.

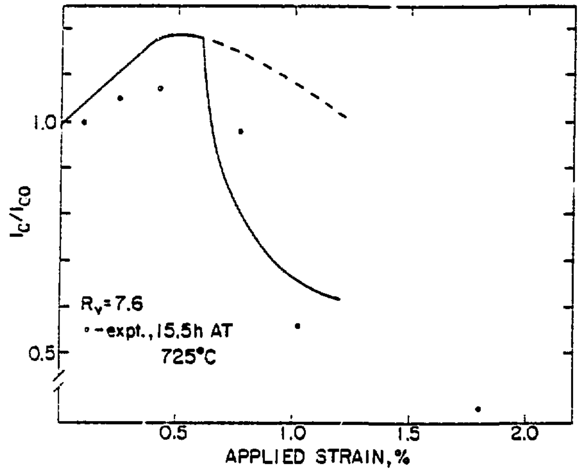

Figure 4. Calculated and observed critical current as a function of applied bending strain. Samples were bent at room temperature and tested for their current carrying capacities at 4.2K and 4T.

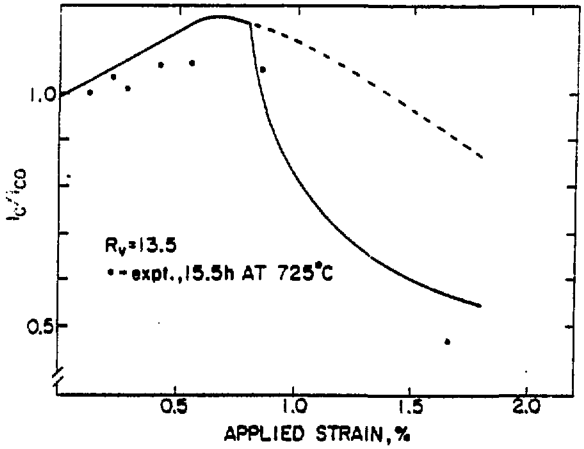

Figure 5. Calculated and observed critical current as a function of applied bending strain. Samples were bent at room temperature and tested for their current carrying capacities at 4.2K and 4T.

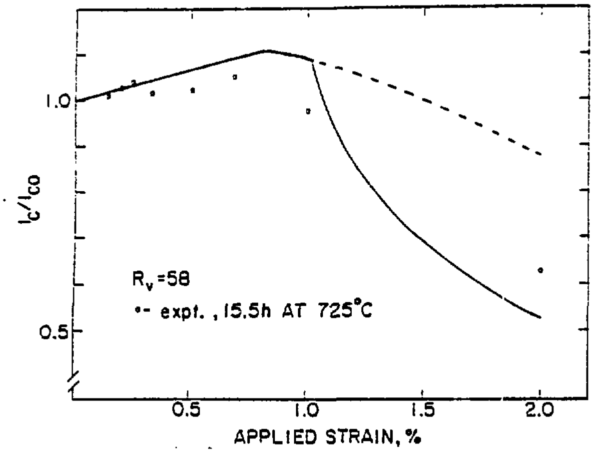

Figure 6. Calculated and observed critical current as a function of applied bending strain. Samples were bent at room temperature and tested for their current carrying capacities at 4.2K and 4T.

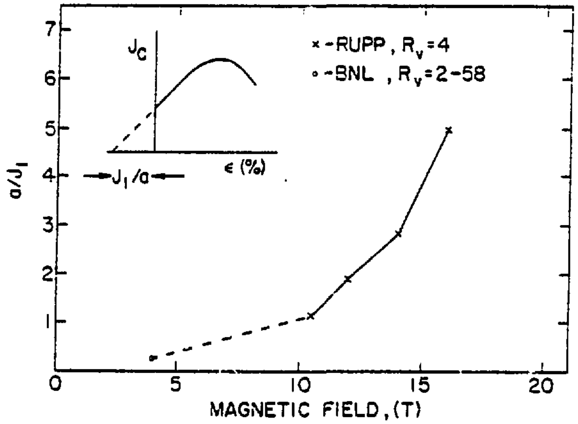

Figure 7. The parameter a/J_1 as a function of applied magnetic field. Crosses taken from reference 4.